Published in Polyhedron, 18, issues 20, 2679-2685, 1999
which should be used for any reference to this work

Cluster build-up in aqueous solution: synthesis, structure, protonation and catalytic properties of the trinuclear cation $[(\eta^6\text{-}C_6H_6)(\eta^6\text{-}C_6Me_6)_2Ru_3(\mu_2\text{-}H)_3(\mu_3\text{-}O)]^+$

Matthieu Faure, Manfred Jahncke, Antonia Neels, Helen Stœckli-Evans, Georg Süss-Fink*

Institut de Chimie, Université de Neuchâtel, CH-2000 Neuchâtel, Switzerland

Received 22 April 1999; accepted 16 June 1999

Abstract

The trinuclear oxo-capped cluster cation $[(\eta^6\text{-}C_6H_6)(\eta^6\text{-}C_6Me_6)_2Ru_3(\mu_2\text{-}H)_3(\mu_3\text{-}O)]^+$ (**2**) was synthesised by reacting $[(\eta^6\text{-}C_6Me_6)Ru(H_2O)_3]^{2+}$ with $[(\eta^6\text{-}C_6Me_6)_2Ru_2(\mu_2\text{-}H)_3]^+$ in aqueous solution. The single-crystal X-ray structure analysis of the tetrafluoroborate salt shows the cation to contain a H_2O molecule hydrogen-bonded to the μ_3-oxo ligand. Acidification experiments show two protonation steps occuring at this H_2O molecule and the oxo cap of the triruthenium cluster. The cluster cation **2** catalyses the hydrogenation of aromatic compounds in aqueous solution under biphasic conditions.

Keywords: Cluster; Trinuclear; Ruthenium; Arene ligand; Oxo cap; Aromatic hydrogenation; Water-soluble catalyst

1. Introduction

Ligand-stabilised transition metal clusters continue to receive much attention due to their fascinating structural properties [1], their significance as models for metal surfaces with chemisorbed molecules attached to them ('cluster-surface-analogy') [2], and to their-sometimes unique-catalytic potential [3]. Most transition metal clusters have been synthesised in a non-systematic manner by allowing the starting complexes to aggregate under thermal or photochemical activation. In contrast to this stands the idea of a rational synthetic approach, which would allow the formation of predictable target molecules with predefined nuclearity [4]. This may be achieved by the addition of mono- or dinuclear fragments to reactive complexes, as exemplified by the reaction of the dinuclear $Co_2(CO)_8$ with the carbyne complex $(\eta^5\text{-}C_5H_5)(CO)_2W{\equiv}C(C_6H_4CH_3\text{-}p)$ giving the trinuclear addition product $(\eta^5\text{-}C_5H_5)WCo_2(CO)_8C(C_6H_4CH_3\text{-}p)$ in which the $C(C_6H_4CH_3\text{-}p)$ group appears as a capping ligand [5].

Previously we have shown that the arene–ruthenium unity represents an organometallic fragment that tends to aggregate to cationic hydrido clusters with up to four metal atoms. These clusters are formed in aqueous solution by treating mononuclear arene–ruthenium complexes with molecular hydrogen. The nuclearity of the products depends crucially on the steric demands of the arene ligands: Thus with the unsubstituted or disubstituted arene ligand the tetranuclear clusters $[(\eta^6\text{-arene})_4Ru_4H_4]^{2+}$ and $[(\eta^6\text{-arene})_4Ru_4H_6]^{2+}$ (arene=benzene, *para*-cymene) are accessible, while with the tetrasubstituted arene ligand 1,2,4,5-tetramethylbenzene the trinuclear hydrido clusters $[(\eta^6\text{-}C_6H_2Me_4)_3Ru_3(\mu_2\text{-}H)_3(\mu_3\text{-}Cl)]^{2+}$ and $[(\eta^6\text{-}C_6H_2Me_4)_3Ru_3(\mu_2\text{-}H)_3(\mu_3\text{-}O)]^+$ are formed [6]. With the *per*-alkylated hexamethylbenzene ligand, finally, the reaction affords the only dinuclear product $[(\eta^6\text{-}C_6Me_6)_2Ru_2(\mu_2\text{-}H)_3]^+$ (**1**) [7], a complex which is best prepared by using an aqueous solution of $NaBH_4$ as hydride donor [8], Scheme 1.

In accordance with its electron-deficiency, represented either by three 2e-3c Ru–H–Ru bonds or by a Ru≡Ru triple bond with three hydrido bridges, **1** shows a high reactivity towards nucleophiles, as observed in the reactions with borohydride salts, hydrazine, pyrazole, and triazoles [8–10]. The objective of this work is to extend the synthetic applications of **1** to rational cluster build-up reactions. Given that, on the one hand, three tetramethylbenzene–ruthenium fragments can be put together

*Corresponding author. Tel.: +41-32-718-2400; fax: +41-32-718-2511.
E-mail address: georg.suess-fink@ich.unine.ch (G. Süss-Fink)

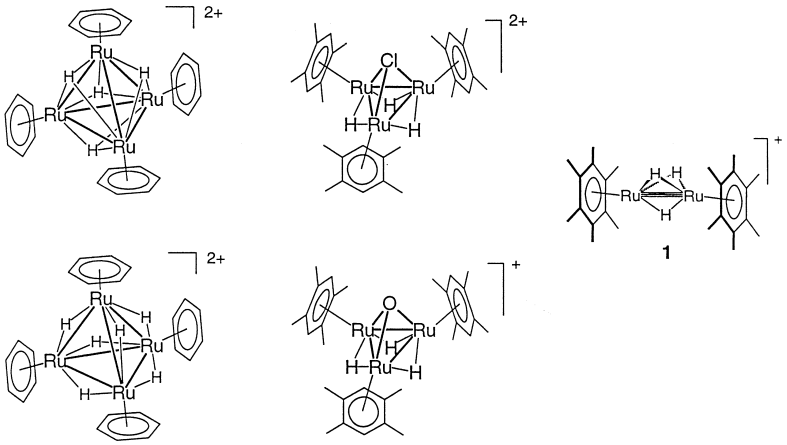

Scheme 1.

to form a trinuclear cluster, whereas, on the other hand, the space left by two hexamethylbenzene–ruthenium fragments is too small for a third hexamethylbenzene–ruthenium fragment, it was tempting to try smaller arene ruthenium fragments for the assembly of unsymmetrically substituted Ru_3 clusters containing two hexamethylbenzene ligands.

2. Results and discussion

The reaction of $[(\eta^6\text{-}C_6Me_6)_2Ru_2(\mu_2\text{-}H)_3]^+$ (**1**) with $[(\eta^6\text{-}C_6H_6)Ru(H_2O)_3]^{2+}$ in aqueous solution results in the formation of the trinuclear cluster $[(\eta^6\text{-}C_6H_6)(\eta^6\text{-}C_6Me_6)_2Ru_3(\mu_2\text{-}H)_3(\mu_3\text{-}O)]^+$ (**2**) according to Eq. (1). In complex **2**, the triruthenium framework is capped by a μ_3-oxo ligand arising from the solvent water. For the reaction according to Eq. (1) the chloro precursor $(\eta^6\text{-}C_6H_6)_2Ru_2Cl_4$ can be employed, which in aqueous solution leads in situ to the triaqua complex $[(\eta^6\text{-}C_6H_6)Ru(H_2O)_3]^{2+}$ [11]. In order to keep the concentration of side-products low, the chloro complex is used in excess, and the reaction is carried out over 3 days at 50°C in neutral solution (pH 6–7). Upon addition of $NaBF_4$, cation **2** precipitates as the tetrafluoroborate salt, Fig. 1.

$$[(\eta^6\text{–}C_6Me_6)_2Ru_2(\mu_2\text{-}H)_3]^+ + [(\eta^6\text{–}C_6H_6)Ru(H_2O)_3]^{2+} \longrightarrow$$

(**1**)

$$[(\eta^6\text{–}C_6H_6)(\eta^6\text{–}C_6Me_6)_2Ru_3(\mu_2\text{-}H)_3(\mu_3\text{-}O)]^+ + 2\ H^+ + 2\ H_2O$$

(**2**)

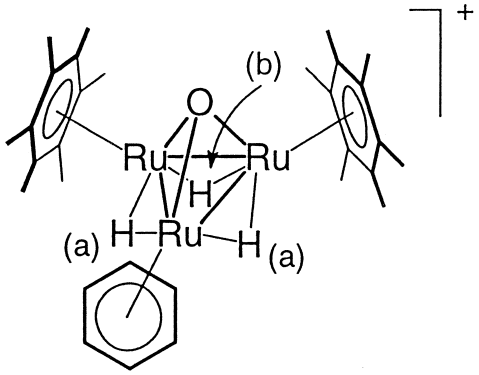

Fig. 1. Assignment of the hydrido ligands in **2**.

Complex **2** is characterised by NMR and IR spectroscopy, mass spectrometry, microanalysis, and a single-crystal X-ray structure analysis. The ^1H NMR spectrum (Table 1) in acetone-d_6 (tetrafluoroborate salt) shows one singlet for the benzene ligand and one singlet for the two hexamethylbenzene ligands. The hydrido ligands appear as a doublet and a triplet in the highfield region. The triangular structure of the $[(\eta^6\text{-}C_6H_6)(\eta^6\text{-}C_6Me_6)_2Ru_3(\mu_2\text{-}H)_3(\mu_3\text{-}O)]^+$-cation can already be deduced from the integration of the NMR signals and from the coupling pattern of the hydrido ligands. The three hydrido ligands in **2** are not fluxional at room temperature, as clearly shown by the two well-resolved highfield signals in the ^1H NMR spectrum of **2**. This compares well to the behaviour of the isoelectronic rhodium complex $[(\eta^5\text{-}C_5Me_5)_3Rh_3(\mu_2\text{-}H)_3(\mu_3\text{-}O)]^+$ [12]. The presence of the oxo ligand and the

Table 1
^1H NMR data [δ] of complex **2** (BF_4-salt) and its protonated forms in acetone-d_6

pH[a]	C_6H_6 (s, 6H)	C_6Me_6 (s, 36H)	H(a) (d, 2H)[c]	H(b) (t, 1H)[c]
3–10[a]	5.70	2.30	−19.08	−19.94
2[a]	5.88	2.38	−18.19	−18.92
0[b]	6.09	2.43	−17.61	−18.19

[a] pH-value of the aqueous solution that was used in order to wash the BF_4-salt of **2** (tuned by use of NaOH or HBF_4).
[b] Addition of one drop of $HBF_4 \cdot Et_2O$ to the acetone-d_6 solution.
[c] $J = 3.7$ Hz.

monocationic charge are revealed by the electrospray mass spectrum (peak centred at m/z 726 with the expected Ru_3-isotope pattern; calculated for ^{102}Ru: 729) and the microanalysis of the tetrafluoroborate salt.

Suitable crystals of the tetrafluoroborate salt of **2** were obtained from an acetone solution upon slow evaporation of the solvent. A single-crystal X-ray structure analysis was performed with one of the orange-red block-shaped crystals. Apart from the cationic complex **2**, the structure of which is depicted in Fig. 2, the BF_4^- anion is found to be disordered with occupancy factors of 0.5 for all fluorine atoms. Selected bond lengths and angles are given in Table 2, Fig. 2.

The structure analysis of **2** confirms the molecule to consist of an equilateral triangle of three ruthenium atoms being capped by a μ_3-oxo ligand. The three hydrido ligands bridging the three ruthenium–ruthenium bonds could be localised and fully refined. Due to the different aromatic ligands the triangular framework is unsymmetrical. The distance between the two ruthenium atoms coordinated to a hexamethylbenzene ring [Ru(1)–Ru(2): 2.7992(6) Å] is slightly longer than the distances between the ruthenium atoms coordinated to two different arene ligands [Ru(1)–Ru(3): 2.7450(6) Å, Ru(2)–Ru(3): 2.7442(6) Å]. Consequently, the bond angle which is centred at the ruthenium atom coordinated by the benzene ligand [Ru(1)–Ru(3)–Ru(2): 61.332(16)°] is larger than those centred at the other two ruthenium atoms [59.353(16)° and 59.325(17)°]. The oxo ligand is symmetrically coordinated over the Ru_3 triangle, the three ruthenium–oxygen distances being almost equal (mean 2.00 Å). Two analogues of **2** have been described, namely

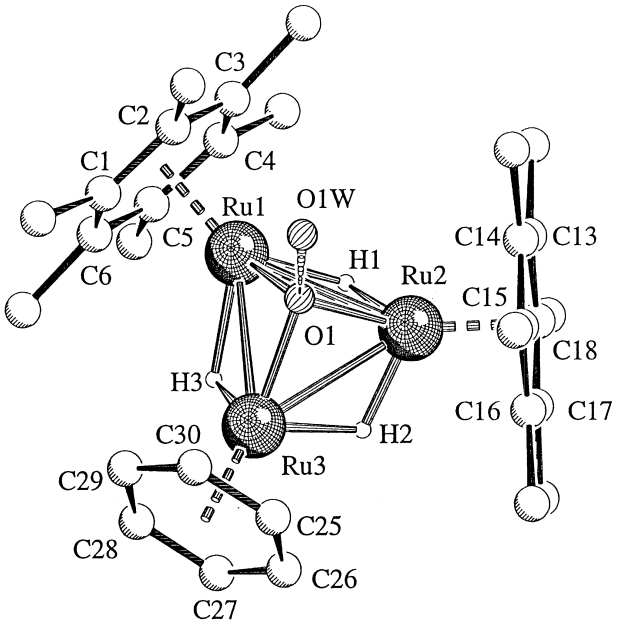

Fig. 2. Structure of **2**, the hydrogen atoms of the hexamethylbenzene ligand and the benzene ligand have been omitted for clarity.

Table 2
Selected bond lengths [Å] and angles [°] for **2**

Interatomic distances		Ru(2)–C(15)	2.211(5)
Ru(1)–Ru(2)	2.7992(6)	Ru(2)–C(16)	2.220(5)
Ru(2)–Ru(3)	2.7442(6)	Ru(2)–C(17)	2.209(5)
Ru(1)–Ru(3)	2.7450(6)	Ru(2)–C(18)	2.234(5)
Ru(1)–O(1)	1.999(3)	Ru(3)–C(25)	2.202(6)
Ru(2)–O(1)	2.003(3)	Ru(3)–C(26)	2.184(7)
Ru(3)–O(1)	2.008(3)	Ru(3)–C(27)	2.198(7)
Ru(1)–H(1)	1.71(4)	Ru(3)–C(28)	2.196(6)
Ru(1)–H(3)	1.88(6)	Ru(3)–C(29)	2.213(6)
Ru(2)–H(1)	1.69(4)	Ru(3)–C(30)	2.195(6)
Ru(2)–H(2)	1.56(8)		
Ru(3)–H(2)	1.76(7)	Hydrogen bond	
Ru(3)–H(3)	1.71(6)	O(1)–O(1W)	2.853(1)
Ru(1)–C(1)	2.222(5)		
Ru(1)–C(2)	2.200(5)	Bond angles	
Ru(1)–C(3)	2.216(6)	Ru(1)–Ru(2)–Ru(3)	59.353(16)
Ru(1)–C(4)	2.213(5)	Ru(1)–Ru(3)–Ru(2)	61.322(16)
Ru(1)–C(5)	2.241(5)	Ru(3)–Ru(1)–Ru(2)	59.325(17)
Ru(1)–C(6)	2.200(5)	Ru(1)–O(1)–Ru(2)	88.78(12)
Ru(2)–C(13)	2.231(5)	Ru(1)–O(1)–Ru(3)	86.49(12)
Ru(2)–C(14)	2.206(5)	Ru(2)–O(1)–Ru(3)	86.36(12)

the isoelectronic pentamethylcyclopentadienyl–rhodium complex $[(\eta^5\text{-}C_5Me_5)_3Rh_3(\mu_2\text{-}H)_3(\mu_3\text{-}O)]^+$ [12] and the tetramethylbenzene–ruthenium complex $[(\eta^6\text{-}C_6H_2Me_4)_3Ru_3(\mu_2\text{-}H)_3(\mu_3\text{-}O)]^+$ [6]. Complex **2** is the first in this series, which has different aromatic ligands, Table 2.

Above the oxo ligand of **2**, a second oxygen belonging to a water molecule is bound with an O–O distance of 2.853(1) Å. This water molecule is hydrogen-bonded to the μ_3-oxo cap and cannot be removed by prolongated drying in high vacuum. The isoelectronic cation $[(\eta^5\text{-}C_5Me_5)_3Rh_3(\mu_2\text{-}H)_3(\mu_3\text{-}O)]^+$ [12] also crystallises with a water molecule bound to the oxo ligand, while the tris(1,2,4,5-tetramethylbenzene) analogue $[(\eta^6\text{-}C_6H_2Me_4)_3Ru_3(\mu_2\text{-}H)_3(\mu_3\text{-}O)]^+$ crystallises even as a dihydrate [6], Table 1.

The protonation of cation **2** with $HBF_4\cdot Et_2O$ has been studied by ^{1}H NMR spectroscopy. In acetone-d_6 two successive steps of protonation can be distinguished: The first protonation step is observed in the pH range from 4 to 2, the second one in the range from 1 to 0, Scheme 2.

From the fact that the coupling patterns of the four signals [(η^6-C_6H_6), (η^6-C_6Me_6), H(a), H(b)] do not change upon protonation, it can be deduced that the protonation does neither occur at the Ru_3-framework nor at one of the arene ligands. The only remaining possible site of protonation is the μ_3-oxo ligand, which functions as a 4e donor and has a free electron pair. However, this could explain the first step of protonation, but not the second one. In order to account for the two protonation steps observed, we have to consider the water molecule attached by hydrogen bonds to the μ_3-oxo cap in **2**, observed by the single-crystal X-ray structure analysis of $[(\eta^6\text{-}C_6H_6)(\eta^6\text{-}C_6Me_6)_2Ru_3(\mu_2\text{-}H)_3(\mu_3\text{-}O)][BF_4]$. We assume that, in the

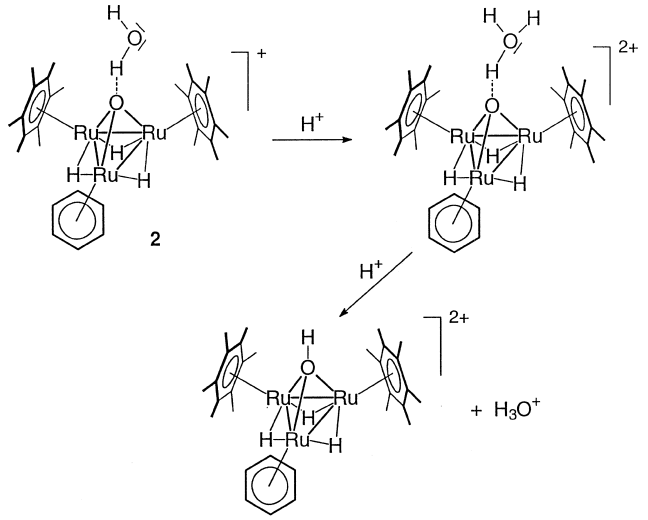

Scheme 2.

first protonation step this water molecule is protonated to give a hydronium cation still hydrogen bonded to the oxo ligand. The second proton is assumed to attack the hydronium molecule with cleavage of the hydrogen bond which leads to a μ_3-hydroxo ligand (Scheme 2).

The cluster cation **2** was found to catalyse the hydrogenation of benzene and various benzene derivatives in aqueous solution to give the corresponding cyclohexane derivatives. The aromatic substrates are hydrogenated with molecular hydrogen (60 bars) at 110°C with vigorous stirring of the biphasic system. The trinuclear cluster cation **2** can be recovered unchanged in each case as the tetrafluoroborate salt after a catalytic run from the aqueous phase, Eq. (2).

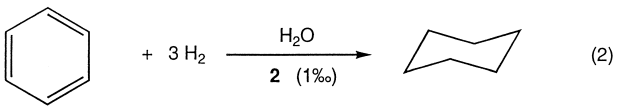

(2)

For benzene, the reaction is almost complete within 3 h, the catalytic turnover frequency being 289 h^{-1}. Toluene is hydrogenated faster than benzene, presumably due to the increased electronic density of the aromatic cycle. This electronic effect, however, is counter-balanced by steric effects which increase with the increasing steric bulk of the substituents: Therefore the TOF decreases for the benzene derivatives with bulky substituents (Table 3). In accordance with these electronic and steric trends, anisole shows a low TOF, despite little steric hindrance, because of the electron-withdrawing effect of the methoxy substituent. The exceptionally high TOF for cyclohexylbenzene can presumably be explained by the better miscibility of the aqueous and organic phases due to the density of cyclohexylbenzene similar to that of the water (Tables 3–5).

The same tendencies are observed with di-, tri- and tetrasubstituted benzene derivatives. The sterically less hindered *para*-xylene is more easily hydrogenated than the *meta* derivative, while the more hindered *ortho* derivative is more difficult to hydrogenate. The tetramethylsubstituted benzene shows the lowest TOF value (Table 4).

The hydrogenation of benzene derivatives with **2** in aqueous solution is not very selective: In addition to the hydrogenation of the aromatic ring, reducible functions of the substituents are also hydrogenated. Thus, styrene gives mainly ethylbenzene and some ethylcyclohexane (Table 5). In the case of phenylacetylene, mainly ethylbenzene and ethylcyclohexane are obtained after 3 h, while after 2 h ethylbenzene is the major product and traces of styrene are observed. This clearly shows that the triple bond is faster hydrogenated than the double bond, while the aromatic ring is hydrogenated with lower activity. The hydrogenation of aromatic compounds, catalysed by **2** in aqueous solution, is tolerant to acidic and basic functions: Thus, aniline as well as phenol are hydrogenated to give the corresponding cyclohexane derivatives. However, addition of a strong acid such as HNO_3 (pH 2) blocks the catalytic activity. This desactivation of the catalyst is presumably due to the protonation of the oxo cap in cation **2** (Scheme 2).

Table 3
Hydrogenation of benzene and monosubstituted derivatives under biphasic conditions[a]

Substrate	Product	Yield (%)[b]	Time (h)	TON[c]	TOF (h^{-1})[d]
Benzene	Cyclohexane	96.1	3.5	961	289
Toluene	Methylcyclohexane	95.0	2.2	950	440
Propylbenzene	Propylcyclohexane	94.0	8.0	967	117
Isopropylbenzene	Isopropylcyclohexane	98.8	14.0	988	71
Butylbenzene	Butylcyclohexane	98.6	14.0	986	70
Cyclohexylbenzene	Bicyclohexyl	100.0	2.0	1000	500
Biphenyl[e]	Bicyclohexyl	99.6	14.5	996	68
Anisole	Methoxycyclohexane	81.9	11.0	819	74

[a] Conditions: catalyst $[(\eta^6\text{-}C_6H_6)(\eta^6\text{-}C_6Me_6)_2Ru_3(\mu_2\text{-}H)_3(\mu_3\text{-}O)][BF_4]$ (0.01 mmol), catalyst/substrate ratio 1/1000, temperature 110°C, hydrogen pressure 60 bars, stirred at 900 min^{-1}.

[b] Measured by gas chromatography.

[c] Catalytic turnover: mol substrate transformed per mol catalyst.

[d] Catalytic turnover frequency: mol substrate transformed per mol catalyst per time unit (h^{-1}).

[e] Substrate dissolved in cyclohexane (10 ml).

Table 4
Hydrogenation of di-, tri- and tetrasubstituted derivatives under biphasic conditions[a]

Substrate	Product	Yield (%)[b]	Time (h)	TON[c]	TOF (h^{-1})[d]
o-Xylene	*trans*-1,2-Dimethylcyclohexane	13.6	14.0	995	71
	cis-1,2-Dimethylcyclohexane	85.9			
m-Xylene	*trans*-1,3-Dimethylcyclohexane	20.4	3.0	994	232
	cis-1,3-Dimethylcyclohexane	79.0			
p-Xylene	*trans*-1,4-Dimethylcyclohexane	31.0	2.0	990	396
	cis-1,4-Dimethylcyclohexane	68.0			
1,3,5-Trimethyl-benzene	*trans,trans*-1,3,5-Trimethylcyclohexane	19.2	14.0	989	71
	cis,cis-1,3,5-Trimethylcyclohexane	79.7			
1,2,4,5-Tetramethyl-benzene[e]	*trans,trans,trans*-1,2,4,5-Tetramethyl-cyclohexane	1.9	14.0	34	1.4
	cis,cis,cis-1,2,4,5-Tetramethyl-cyclohexane	1.4			

[a] Conditions: catalyst $[(\eta^6\text{-}C_6H_6)(\eta^6\text{-}C_6Me_6)_2Ru_3(\mu_2\text{-}H)_3(\mu_3\text{-}O)][BF_4]$ (0.01 mmol), catalyst/substrate ratio 1/1000, temperature 110°C, hydrogen pressure 60 bars, stirred at 900 min^{-1}.
[b] Measured by gas chromatography.
[c] Catalytic turnover: mol substrate transformed per mol catalyst.
[d] Catalytic turnover frequency: mol substrate transformed per mol catalyst per time unit (h^{-1}).
[e] Substrate dissolved in cyclohexane (10 ml).

The implication of cluster cation $[(\eta^6\text{-}C_6H_6)(\eta^6\text{-}C_6Me_6)_2Ru_3(\mu_2\text{-}H)_3(\mu_3\text{-}O)]^+$ (**2**) in the catalytic hydrogenation of aromatic substrates is not clear. In no case we observed substitution of the benzene ligand or of a hexamethylbenzene ligand by the aromatic substrate; **2** was always recovered unchanged. This means that the aromatic substrate cannot be coordinated by substitution to one of the ruthenium atoms during the catalytic process. It seems that the aromatic substrate is arranged in a loose contact over the open triangular face of the triruthenium cluster, opposite to the oxo cap, a phenomenon which can be explained by hydrophobic interactions between the aromatic ligand of the cluster and the aromatic substrate in aqueous solution. Similar phenomena are observed in inclusion complexes between benzene–ruthenium units and cyclodextrines [13].

Table 5
Hydrogenation of functionalised benzene derivatives under biphasic conditions[a]

Substrate	Product	Yield (%)[b]	Time (h)	TON[c]	TOF (h^{-1})[d]
Styrene	Ethylbenzene	75.0	3.0	970	323
	Ethylcyclohexane	22.0			
Phenylacetylene	Ethylcyclohexane	26.0	2.0	988	494
	Ethylbenzene	71.8			
	Styrene	1.0			
Phenylacetylene	Ethylcyclohexane	59.8	3.0	1000	333
	Ethylbenzene	40.2			
α-Methylstyrene	Isopropylcyclohexane	99.2	1.5	992	661
Allylbenzene	Propylcyclohexane	96.5	16.5	996	59
Phenol	Cyclohexanol	97.8	14.5	978	68
Acetophenone	1-Cyclohexylethanol	97.8	14.5	978	68
Methylbenzoate	Methylcyclohexanoate	91.5	20.0	983	45
Ethylbenzoate	Ethylcyclohexanoate	70.7	20.0	983	35
Aniline	Cyclohexylamine	62.1	24.0	696	26
α-Methylbenzyl-amine	α-Methylcyclohexyl-amine	2.3	24.0	23	1
N,N-Dimethylaniline	*N,N*-Dimethylcyclohexylamine	1.2	24.0	12	0.5

[a] Conditions: catalyst $[(\eta^6\text{-}C_6H_6)(\eta^6\text{-}C_6Me_6)_2Ru_3(\mu_2\text{-}H)_3(\mu_3\text{-}O)][BF_4]$ (0.01 mmol), catalyst/substrate ratio 1/1000, temperature 110°C, hydrogen pressure 60 bars, stirred at 900 min^{-1}.
[b] Measured by gas chromatography.
[c] Catalytic turnover: mol substrate transformed per mol catalyst.
[d] Catalytic turnover frequency: mol substrate transformed per mol catalyst per time unit (h^{-1}).

3. Experimental

3.1. General

All manipulations were carried out by routine under nitrogen atmosphere, using standard Schlenk techniques, although the compounds are not air-sensitive. The bidistilled water was degassed and saturated with inert gas prior to use. The NMR spectra were recorded on a Varian Gemini 200 BB instrument, the treatment of the spectra was performed using a SUN Varian station. The IR spectra were recorded on a Perkin-Elmer FT-IR 1720 X spectrophotometer (4000–400 cm^{-1}) as KBr pellets. Microanalytical data were obtained from the Mikroelementaranalytisches Laboratorium der ETH Zürich. The electrospray mass spectra were obtained in positive-ion mode with a LCQ Finnigan mass spectrometer using acetone as the mobile phase. The starting materials $(\eta^6\text{-}C_6H_6)_2Ru_2Cl_4$ [14], $(\eta^6\text{-}C_6H_4MePr^i\text{-}p)_2Ru_2Cl_4$ [14], and $(\eta^6\text{-}C_6Me_6)_2Ru_2Cl_4$ [15] were synthesised according to the literature procedures.

3.2. Preparation of $[(\eta^6\text{-}C_6Me_6)_2Ru_2(\mu_2\text{-}H)_3]^+$ (1)

A mixture of $(\eta^6\text{-}C_6Me_6)_2Ru_2Cl_4$ (100 mg, 0.150 mmol) and Ag_2SO_4 (94 mg, 0.300 mmol) in water (20 ml) was stirred in a Schlenk tube for 1 h in the dark (aluminium foil). During this period the mixture was treated several times with ultrasound (~1 min), until the orange solid was completely dissolved. After filtration of the white precipitate (AgCl) to the yellow solution containing $[(\eta^6\text{-}C_6Me_6)Ru(H_2O)_3]^{2+}$ an aqueous solution of $NaBH_4$ (20 mg, 0.529 mmol, 15 ml H_2O) was added dropwise. The colour of the solution turned dark-green after addition of the first drops but eventually became dark red. After filtration, this aqueous solution of $[(\eta^6\text{-}C_6Me_6)_2Ru_2(\mu\text{-}H)_3]^+$ was used in situ without further work-up. For this reason, the molar quantities of **1**-given in parentheses-as well as the yield of complex **2** are based on the quantity of $(\eta^6\text{-}C_6Me_6)_2Ru_2Cl_4$ employed. For the isolation and characterisation of **1** cf. ref. [8] and [10].

3.3. Synthesis of $[(\eta^6\text{-}C_6H_6)(\eta^6\text{-}C_6Me_6)_2Ru_3(\mu_2\text{-}H)_3(\mu_3\text{-}O)]^+$ (2)

The solid substance $(\eta^6\text{-}C_6H_6)_2Ru_2Cl_4$ (70 mg, 0.140 mmol) was added to an aqueous solution of $[(\eta^6\text{-}C_6Me_6)_2Ru_2(\mu\text{-}H)_3]^+$ (**1**) (0.150 mmol, 40 ml H_2O, pH 6–6.5). The mixture was heated to 50°C for 3 days in a closed pressure Schlenk tube. The resulting red solution was filtered and then treated with an aqueous solution of $NaBF_4$ (40 mg ml^{-1}, 2 ml, 0.73 mmol). The orange-red precipitate formed was centrifuged, washed with neutral water (2×5 ml) and dried to give $[(\eta^6\text{-}C_6H_6)(\eta^6\text{-}C_6Me_6)_2Ru_3(\mu_2\text{-}H)_3(\mu_3\text{-}O)][BF_4]$ (cation **2**, 70 mg, 0.084 mmol, 56%). Anal. Calcd for $C_{30}H_{45}B_1F_4O_1Ru_3\cdot H_2O$: C, 43.43; H, 5.71. Found: C, 43.32; H, 5.71. IR (cm^{-1}): 3605 (m), ν(O–H); 3020 (w), $\nu(C\text{–}H_{ar})$; 2920 (m), ν(C–H); 1435 (m), 1385 (m), ν(C=C); 1060 (br, vs), $\nu(BF_4)$; 820 (m).

3.4. X-ray structure determination of complex 2

The X-ray data were recorded using a Stoe Imaging Plate Diffractometer System (IPDS, Stoe & Cie 1995) equipped with a one-circle φ goniometer and a graphite-monochromator, using Mo-Kα radiation ($\lambda = 0.71073$ Å); 200 exposures (3 min per exposure) were obtained at an image plate distance of 70 mm with $0 < \varphi < 200°$ and with the crystal oscillating through 1° in φ, resolution $D_{min} - D_{max}$ 12.45–0.81 Å. Table 6 summarizes the crystallographic and selected experimental data.

The structure was solved by direct methods using the program SHELXS 86 [16] and refined by full-matrix least-squares on F^2 using the program SHELXL 93 [17]. The figure was drawn with SCHAKAL [18]. The hydrido ligands were located from difference maps and fully refined The methyl hydrogens of the hexamethylbenzene ligands and the aromatic hydrogen atoms of the benzene ligand were included in calculated positions and refined as riding atoms using the SHELXL 93 default parameters.

3.5. Catalytic runs

In a typical experiment, 0.01 mmol of **2** (terafluoroborate salt) were dissolved in 5 ml of bidistilled water. To this solution, placed in a 100 ml stainless steel autoclave, 10 mmol of the organic substrate were added. After purging four times with hydrogen, the autoclave was pressured with hydrogen (60 bars) and heated to 110°C in an oil bath under vigorous stirring of the reaction mixture (900 rpm). After the reaction time indicated in Tables 3–5, the autoclave was cooled with ice-water to room temperature, and the pressure was released. The two-phase system was separated by decantation; the aqueous phase was evaporated to dryness, the residue dissolved in D_2O and analysed by NMR spectroscopy, the organic phase containing products and substrates was analysed by CG and NMR spectroscopy.

Supplementary data

Full tables of atomic parameters, bond lengths and angles are deposited at the Cambridge Crystallographic Data Center, 12 Union Road, Cambridge CB2 1EZ, UK (Deposition Number CCDC 118853).

Acknowledgements

We thank the Swiss National Science Foundation for financial support of this work and the Johnson Matthey

Table 6
Crystallographic and selected experimental data for **2**

Compound	$[(\eta^6\text{-}C_6H_6)(\eta^6\text{-}C_6Me_6)_2Ru_3(\mu_2\text{-}H)_3(\mu_3\text{-}O)][BF_4]$ (cation **2**)
Formula	$C_{30}H_{45}B_1F_4O_1Ru_3\cdot H_2O$
Crystal colour	red-orange
Crystal shape	block
Crystal size/mm^3	$0.40\times0.30\times0.10$
M_r/g mol^{-1}	829.70
Crystal system	triclinic
Space group	$P\bar{1}$
a/Å	10.848(9)
b/Å	10.922(3)
c/Å	14.041(4)
α/°	96.14(0)
β/°	96.57(6)
γ/°	104.57(5)
V/Å^3	1583.7(3)
Z	2
D_c/g cm^{-3}	1.740
μ (Mo K_α)/mm^{-1}	1.461
F(000)	832
θ Scan-range/°	2.27–25.85
T/K	293(2)
Reflections measured	12452
Independent reflections	5716
Reflections observed [$I>2\sigma(I)$]	4413
Final R indices [$I>2\sigma(I)$][a]	$R_1=0.0365$, $wR_2=0.0888$
R-Indices (al data)[a]	$R_1=0.0497$, $wR_2=0.0969$
Goodness of fit	0.940
Maximum Δ/σ	0.001
Residual density: maximum, minimum $\Delta\rho$/e Å^{-3}	+0.848, −1.092

[a] $R_1=\Sigma\ ||F_0|-|F_c||/\Sigma\ |F_0|$, $wR_2=[\Sigma\ w(F_0^2-F_c^2)^2/\Sigma\ (wF_0^4)]^{1/2}$.

Research Centre for a generous loan of ruthenium(III) chloride hydrate.

References

[1] C.E. Housecroft, in: Cluster Molecules of the p-Block Elements, Oxford University Press, Oxford, 1994.
[2] E.L. Muetterties, T.N. Rhdoin, E. Band, C.F. Brucker, W.R. Pretzer, Chem. Rev. 79 (1979) 97.
[3] G. Süss-Fink, M. Jahncke, in: R.D. Adams, F.A. Cotton (Eds.), Catalysis by Di- and Polynuclear Metal Cluster Complexes, Wiley-VCH, New York, 1998, p. 167.
[4] G.L. Geoffroy, in: B.C. Gates, L. Guczi, H. Knözinger (Eds.), Metal Clusters in Catalysis, Elsevier, Amsterdam, 1986, p. 1.
[5] M.J. Chetcuti, P.A.M. Chetcuti, J.C. Jeffery, R.M. Mills, P. Mitrprachachon, S.J. Pickering, F.G.A. Stone, D. Woodward, J. Chem. Soc., Dalton Trans. (1982) 699.
[6] G. Meister, G. Rheinwald, H. Stœckli-Evans, G. Süss-Fink, J. Chem. Soc., Dalton Trans. (1994) 3215.
[7] M. Jahncke, Ph.D. Thesis, University of Neuchâtel, Switzerland, 1998.
[8] M. Jahncke, G. Meister, G. Rheinwald, H. Stœckli-Evans, G. Süss-Fink, Organometallics 16 (1997) 1137.
[9] M. Jahncke, A. Neels, H. Stœckli-Evans, G. Süss-Fink, J. Organomet. Chem. 565 (1998) 97.
[10] M. Jahncke, A. Neels, H. Stœckli-Evans, G. Süss-Fink, J. Organomet. Chem. 561 (1998) 227.
[11] D.R. Robertson, T.A. Stephenson, T. Arthur, J. Organomet. Chem. 162 (1978) 121.
[12] A. Nutton, P. Bailey, P.M. Maitlis, J. Organomet. Chem. 213 (1981) 313.
[13] G. Meister, H. Stoeckli-Evans, G. Süss-Fink, J. Organomet. Chem. 453 (1993) 253.
[14] M.A. Bennett, T.-N. Huang, T.W. Matheson, A.K. Smith, Inorg. Synth. 21 (1982) 74.
[15] T. Arthur, T.A. Stephenson, J. Organomet. Chem. 208 (1981) 369.
[16] G.M. Sheldrick, SHELXS 86, Acta Crystallogr., Sect. A 46 (1990) 467.
[17] G.M. Sheldrick, SHELXL 93 A program for crystal structure refinement, University of Göttingen, Göttingen, Germany, 1993.
[18] E. Keller, SCHAKAL 92/V256 A Fortran program for the graphical representation of molecular and crystallographic models, University of Freiburg, Germany, 1992.